Two-Tier Energy Compensation Framework Based on Mobile Vehicular Electric Storage

Nan Chen, *Student Member, IEEE*, Jinghuan Ma, Miao Wang, *Member, IEEE*, and Xuemin Shen, *Fellow, IEEE*

***Abstract*—Plug-in electric vehicle (PEV) commercialization propels an extensive charging station deployment in a power distribution system to satisfy fast growing PEV charging demands. Considering the power distribution, some stations deployed at limited capacity feeders may undergo power overload at peak hours due to time-varying traffic and PEV demands. The potential power overload could lead to severe transformer degradation or even black-out on the aged power infrastructure. To avoid power overload without excessive expenditure on the infrastructure upgrade, proper energy compensation at limited capacity station is highly effective. In this paper, we investigate an energy compensation problem based on utility-owned mobile vehicular electric storage (MVES), aiming to mitigate the overload issues among a group of charging stations (GCS). First, a Markov Chain based energy capacity model is developed to estimate the energy statuses among GCS and a graph theory based GCS transportation model is developed to facilitate on-road MVES allocation. Then, a two-tier energy compensation framework is introduced to efficiently schedule MVESs to minimize the scheduling cost. Simulations are conducted based on real traffic data on California highway collected by California department of transportation, and the results validate the effectiveness of the introduced framework.**

***Index Terms*—Plug-in electric vehicle, energy compensation framework, mobile vehicular electric storage, charging station.**

NOMENCLATURE

$\alpha_{\mathrm{r_e},1}$	Energy charging price fluctuation causing by the demanding energy deviation from the primary price setting.
$\alpha_{\mathrm{r_e},2}$	Primary price setting without energy fluctuation.
$\alpha_{\mathrm{r_e},3}$	Energy charging price basis.
β	Transportation price per km per kWh.
$\Delta E_{\mathrm{av.}}$	The average MVES discharging capacity.
$\lambda_{\mathrm{PEV,h}}$	The on-road PEV traffic flow at time h.
$\lambda_{\mathrm{s,h}}$	The PEV arrival rate at station s at time h.
$\lambda_{\mathrm{sM,h}}$	The average arrival rate of MVESs at station s at time h.
μ_{s}	The service rate of station s.
π	The steady-state probability of Markov Chain.
$\rho_{\mathrm{s,h}}$	The percentage of arriving PEVs at station s at time h.
a	The overall number of PEVs being served in the station.
b	The number of PEVs being served by MVESs.
$C_{\mathrm{charge,h}}$	The cost of charging MVESs at resourceful station at time h.
$C_{\mathrm{charge,r_e,h}}$	Energy charging price at station r_{e} at time h.
C_{h}	Overall scheduling cost at time h.
$C_{\mathrm{Mq_f,h}}$	The energy capacity of station q_{f} provided by MVESs at time h.
$C_{\mathrm{Mr_e,h}}$	The MVES charging capacity of station r_{e} at time h.
C_{sL}	The energy capacity of station s provided by local feeder.
$C_{\mathrm{trans,h}}$	The transportation cost during MVES energy transmission process at time h.
$D_{\mathrm{z_n z_m}}$	The distance between road intersections z_{n} and z_{m}.
e	an all one vector of length of l.
$E_{\mathrm{q_f,k,h}}$	The energy discharged by the kth MVES coming to station q_{f} during time h.
$E_{\mathrm{r_e,q_f,h}}$	The energy transmitted from stations r_{e} to q_{f} at time h.
Ed	Traffic routes as graph edges.
$G(V, Ed)$	A directed graph.
$g_{\mathrm{s,h}}$	The MVES energy supply rate at station s at time h.
h	The time of the day.
i, j	The row/column of the Markov Chain.
l	The total number of elements in Markov Chain.
$L_{\mathrm{av.}}$	The average PEV charging demand.
M	The transition matrix of Markov Chain.

Manuscript received January 24, 2018; revised June 14, 2018; accepted September 19, 2018. Date of publication October 4, 2018; date of current version December 14, 2018. The review of this paper was coordinated by Prof. M. Khodayar. *(Corresponding author: Nan Chen.)*

N. Chen and X. Shen are with the Department of Electrical and Computer Engineering, University of Waterloo, Waterloo, ON N2L 3G1 Canada (e-mail: n37chen@gmail.com; sshen@uwaterloo.ca).

J. Ma is with the School of Electronics Engineering and Computer Science, Peking University, Beijing 100871, China (e-mail: mjhdtc@pku.edu.cn).

M. Wang is with the Department of Electrical and Computer Engineering, Miami University College of Engineering and Computing, Oxford, OH 45056 USA (e-mail: miaowang.buaa@gmail.com).

Color versions of one or more of the figures in this paper are available online at http://ieeexplore.ieee.org.

Digital Object Identifier 10.1109/TVT.2018.2874046

m_{ij}	The ith row, jth column element in Markov Chain.
$N_{\mathrm{q_f M,h}}$	The number of PEVs charged by MVESs at station q_{f} at time h.
N_{sL}	The number of PEVs charged by local feeder at station s.
$p_{\mathrm{availability}/}$ $p_{\mathrm{unavailability,s,h}}$	The station availability/unavailability of. station s at time h.
$P_{\mathrm{C,s}}$	The adopted charging standard at station s.
$p_{\mathrm{QoS,s}}$	The pre-defined station availability at station s.
$P_{\mathrm{s,L}}$	The power capacity of local feeder connected to station s.
Q	The set of limited capacity stations.
q_{f}	The fth limited capacity station in Q.
R	The set of resourceful stations.
r_{e}	The eth resourceful station in R.
$R_{\mathrm{s,h}}$	PEV charging demand at station s, time h.
S	The set of GCS.
s	A charging station in s.
$S_{\mathrm{z_n z_m}}$	The route between road intersections z_{n} and z_{m}.
$t_{\mathrm{z_n z_m}}$	The travel time between road intersections z_{n} and z_{m}.
V	Road intersections as vertex.
V	Road intersections as vertexes.
$v_{\mathrm{z_n z_m}}$	The road velocity between road intersections z_{n} and z_{m}.
Z	The set of road intersections.
z_{g}	The gth road intersection in Z.

I. Introduction

As NUMEROUS government incentive policies launch globally to promote plug-in electric vehicle (PEV) commercialization [1], [2], the PEV will inevitably dominate in the vehicle market. Correspondingly, an extensive deployment of charging stations in power distribution system is expected to provide satisfactory charging service. From a sustainable developing perspective, the implementation of this huge project will mainly rely on existing power facilities with a necessary upgrade. Specifically, a portion of the charging stations are expected to be deployed at the primary feeders, served to guarantee sufficient loading capacities around 2MW at a high voltage level between 4 to 35 kV [3], [4]. On the other hand, to complement the energy supply where the primary feeders cannot reach out, some charging stations are deployed at the secondary feeders, of which the voltage decreases to a lower level between 100 to 240 V and the loading capacity to a hundred-kW level [4].

With the hierarchical deployment, adjacent charging stations can be clustered together as a group of charging stations (GCS) with different energy capacities with respect to local charging demands. Considering the time-varying geographic distribution of PEV traffic loads [5], [6], an intuitive concern raised by local utilities and distribution companies is that power shortage may occur at some of the stations in a GCS. Those overloaded feeders could encounter severe transformer degradation, power quality degradation, or even local black-out [7], [8]. Thus, the power grid urgently demands cost-efficient and fast-response energy storages to help alleviate the power shortage while avoiding excessive expenditure on upgrade. This requirement can be abstracted as how to reallocate the energy resources to a group of service nodes beyond their inherent limits in respond to the real-time demand distribution.

A possible solution is to utilize mobile energy storages as resource porters to carry resources from resourceful stations to those in shortage. We could refer to the oil tank truck and rethink from the features of PEVs. The PEV battery not only stores energy to support vehicle travelling, but also has a potential in flexible energy delivery [9]. Therefore, in this paper, we utilize the on-road PEV as a flexible energy storage device to compensate the limited energy capacities in some of the charging stations to mitigate the load impact on power system. In terms of the functionality to deliver supplementary electric energy, PEVs that can deliver supplementary energy to the charging stations in power shortage are referred as mobile vehicular electric storage (MVES). An essential technical support of the MVES is the vehicle-to-grid (V2G) technology where PEVs send back energy to the power grid. Existing works on V2G can be classified into renewable energy integration, regulation service provision, and peak load mitigation. By utilizing PEVs as energy buffers to levelize the stochastic renewable energy output, renewable energy can be smoothly integrated into the power system [10]. V2G can also be applied in regulation service to fine tune the frequency and voltage deviation due to the power imbalance [10]. The capacity estimations based on PEV stochasticity for V2G frequency regulation have been studied in [11], [12]. The works in [13], [14] thoroughly study the scheduling schemes to maximize the PEV profit in the regulation market. V2G also extends the PEV functionality to mitigating the peak loads in the work [15] through an energy delivery scheme. To address the PEV random driving behaviours, [16], [17] utilize cloud computing and fuzzy heuristic prediction methods respectively to estimate the PEV mitigation capacity. By integrating V2G technology into PEV mobility, we can make the PEV a flexible mobile energy delivery tool to fulfill the intended goal.

In this paper, we study a energy compensation problem that utilizes MVESs as flexible energy porters via V2G technology. Belonging to the local power utility company, MVESs are large battery-capacity PEVs that specialized in being recharged with additional energy at nearby available resourceful stations, and then deliver the energy to overloaded stations in their peak hours. Since the charging demands are strongly correlated to the on-road traffic condition, the service requests modelling at the charging stations should consider the stochasticity of PEV traffics. In terms of power balance at a charging station, the heterogeneity of arriving PEV State-of-Charge (SoC) also af-

fects the station dynamics over time. From the resource allocation perspective, energy demands need to be satisfied while minimizing the MVES scheduling cost and enhancing the time-efficiency of energy transmission. In this problem, the challenge can be abstracted as how to allocate the MVES energy distribution and transportation route among a GCS to balance the power and minimize the scheduling cost.

In this paper, we introduce a two-tier energy compensation framework that efficiently allocates MVES energy distribution and transportation route among a GCS to avoid overload issues. Upon our knowledge, few research works have utilized MVES as a utility-scaled energy storage device to address the PEV charging overload issue. The main contributions of the paper are listed as below:

1) To characterize the charging and discharging processes at resourceful and limited capacity station respectively, a system model is developed to normalize the operation dynamics on both power and transportation levels;
2) Consider the heterogeneity of input data, a two-tier energy compensation framework is introduced to effectively schedule MVESs among the GCS;
3) To balance the power condition and improve the operation performance (e.g. station availability) among a GCS, an optimization problem is formulated to minimize the scheduling cost while guaranteeing power balance and energy transmission time-efficiency;
4) Using the real traffic data on California highway collected from California department of transportation, simulations are conducted to validate the effectiveness of the introduced framework. The potential influences of technical development and station requirement on scheduling results are also discussed.

The remainder of the paper is organized as follows. The related works are reviewed in Section II. The system model is developed to characterize station operations in Section III. Energy compensation framework is introduced in Section IV. To minimize the scheduling cost, an optimization problem is formulated and solved in Section V. Section VI presents the simulation setup and results, and Section VII summarizes the paper.

II. Related Work

In literature, several research works have investigated utilizing PEV mobility to enable system power balance [18]–[21]. The vehicle-to-vehicle charging is investigated in [20] by encouraging on-road PEVs discharging their surplus energy to relieve the overload issue of PEV charging via price mechanism and advanced communication architecture. Consider the PEV range anxiety issue, the vehicle-to-vehicle method proposed in [20] has a high risk of power imbalance due to its limited energy capacity. Consequently, the energy network concept of using PEVs as energy porters to deliver energy from renewable energy sources to charging stations is proposed in the work [18]. Based on the concept, the work in [19] proposes a minimum cost flow algorithm to plan the energy transportation routes among the energy network. The mobile PEV concept is further used in the work [21] by designing a simple dispatching scheme using mobile charging stations to decrease the PEV charging waiting time in stationary stations.

In general, the reviewed works either use the existing energy in PEVs as additional energy source, or consider PEVs as energy porters to transmit additional energy. However, PEVs' potentials of mitigating PEV charging overload remain open. The goal of this paper is to develop an energy compensation scheme that uses MVESs to effectively mitigate the overload issues timely and cost-efficiently. The incorporation of GCS operation modelling and a two-tier energy compensation framework guarantees a predictable and timely energy balance among GCS with minimal cost.

III. System Model

In this section, station energy capacity model from the power perspective is first defined. Operation dynamics of each station are characterized to analyze the power balance status. Then, the transportation network is abstracted as a directed graph to plan MVES travel routes between stations.

As shown in Fig. 1, we consider a group of PEV charging stations S that are deployed at different levels in a power system, while central controller deployed on top of the power system to control the scheduling activity.

In terms of energy capacity, the charging stations S can be categorized into two classes: R and Q. The first one is resourceful stations, whose set is denoted by $R = \{r_1, r_2 \dots r_{\mathrm{e}}\}$. They are connected to primary feeders with stable and sufficient power supplement from the bulk generations. Different from resourceful stations, limited capacity stations, represented as q_{f}, where $Q = \{q_1, q_2 \dots q_{\mathrm{f}}\}$ are connected to secondary feeders in the remote areas. The resourceful stations are designed with an excessive energy capacity to cope with the peak EV charging hours in a day, whose redundant charging capacity can be used to charge the MVESs. On the other hand, the limited energy capacity, due to limited feeder capacity or limited local power source, can incur overload issues during peak hours. Thus, MVESs can provide limited capacity stations with additional energy to mitigate overload issues.

A. Station Energy Capacity Characterization

The local energy capacity of station s that depends on the feeder capacity, is denoted as C_{sL}. In each station, C_{sL} is further characterized as the number of PEV charging services that the local feeder can provide simultaneously during an hour period. The average PEV charging demand $L_{\mathrm{av.}}$ is defined as 15 kWh, 50% battery capacity of the retailed PEVs, Nissan Leaf [24]. Considering that the station connected feeder has a power capacity of $P_{\mathrm{s,L}}$, the number of PEVs charged by the local power

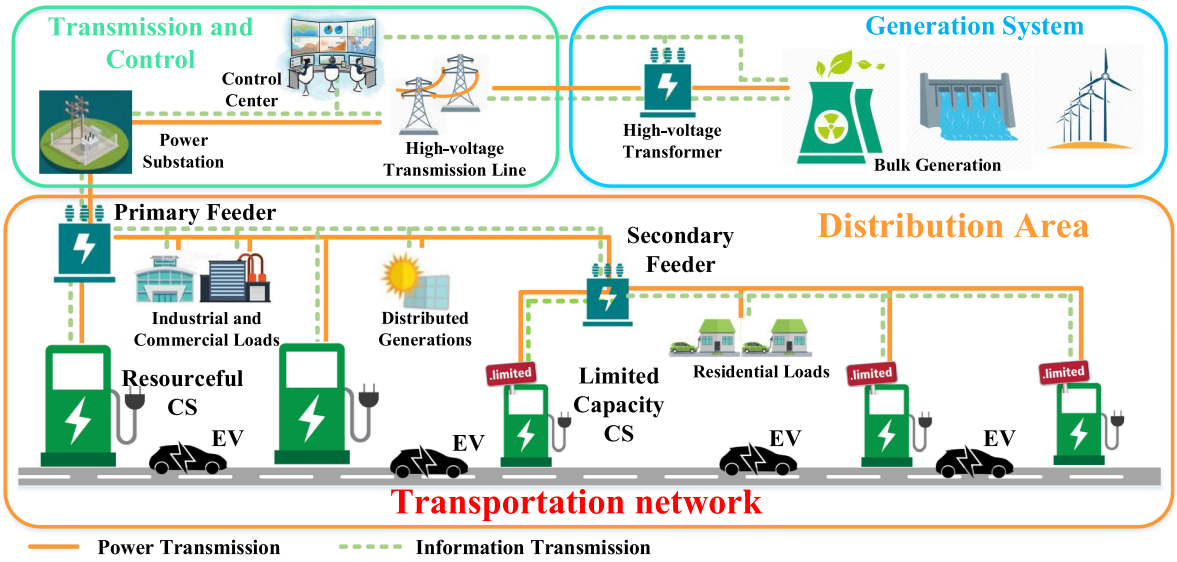

Fig. 1. System overview of the GCS.

denoted as N_{sL} satisfies

$$C_{\mathrm{sL}} = \int_h P_{\mathrm{s,L}} dt = N_{\mathrm{sL}} \cdot L_{\mathrm{av.}}. \tag{1}$$

In terms of the hourly on-road traffic flows, PEV charging demands at station s, denoted as $R_{\mathrm{s,h}}$ is time-variant. Regarding the relation between C_{sL} and $R_{\mathrm{r_e,h}}$, stations from different class response differently. Enabled with sufficient power supplement, resourceful stations can easily fulfill incoming PEV charging demands, denoted as:

$$C_{\mathrm{r_eL}} \geq R_{\mathrm{r_e,h}}. \tag{2}$$

On the other hand, limited capacity stations may encounter power imbalance issues at peak traffic hours, as:

$$C_{\mathrm{q_fL}} \leq R_{\mathrm{q_f,h}}. \tag{3}$$

To address the power imbalance in the limited capacity stations, MVES energy capacity $C_{\mathrm{Mq_f,h}}$ at station q_{f} should complement the energy gap between local energy capacity and PEV charging demands:

$$C_{\mathrm{Mq_f,h}} + C_{\mathrm{q_fL}} \geq R_{\mathrm{q_f,h}} \tag{4}$$

MVESs' energy capacity is the summation of all the MVES discharging energy at the station during hour h. The number of PEVs that are charged by the MVES energy $N_{\mathrm{q_fM,h}}$ can be characterized as:

$$C_{\mathrm{Mq_f,h}} = \sum_k E_{\mathrm{q_f,k,h}} = N_{\mathrm{q_fM,h}} \cdot L_{\mathrm{av.}}, \tag{5}$$

where $E_{\mathrm{q_f,k,h}}$ denotes the energy discharged by the kth MVES coming to station q_{f} during time h. On the other hand, resourceful stations need to undertake the MVES charging tasks besides charging PEVs. The MVES energy capacity in resourceful station r_{e}, denoted as $C_{\mathrm{Mr_e,h}}$, needs to satisfy:

$$C_{\mathrm{r_eL}} \geq C_{\mathrm{Mr_e,h}} + R_{\mathrm{r_e,h}}. \tag{6}$$

B. Station Dynamic Model

By introducing MVESs as energy porters into the power system, dynamics of charging stations require detailed analysis to enable smooth operations. The station dynamics are analyzed on an hourly basis to estimate the average power balance status during hour h, where $h \in [0, 1, 2...22, 23]$ [22].

The station dynamics are characterized as the continuous-time Markov Chain. In terms of the station functionality, the modellings of resourceful and limited capacity stations will be introduced respectively.

1) Limited Capacity Station: In the limited capacity station, two types of vehicles arrive at the station with stochastic property: PEVs for charging and MVESs for energy supplement.

The PEV behaviour can be characterized as a stochastic process, which is based on the following assumptions.

Assumption 1: PEVs arrive at the charging station s following a Poisson process with an average arrival rate of $\lambda_{\mathrm{s,h}}$ at time h.

As validated in [23], the arrival distribution of vehicles at stations follows a Poisson process since each vehicle arrives at stations independently and memorylessly. Hence, in our model, PEVs are considered to follow the Poisson process. The average arrival rate $\lambda_{\mathrm{s,h}}$ depends on the on-road PEV traffic flow $\lambda_{\mathrm{PEV,h}}$, the time h of a day, and the PEV arriving percentage at the station $\rho_{\mathrm{s,h}}$ as

$$\lambda_{\mathrm{s,h}} = \lambda_{\mathrm{PEV,h}} \cdot \rho_{\mathrm{s,h}}. \tag{7}$$

Different from PEVs, MVESs are another independent set of vehicles functioning sorely as energy storage devices. As part of on-road traffics, MVESs have the similar arrival distribution as the PEVs, characterized as the Poisson process as follow.

Assumption 2: MVESs arrive at the charging station s following a Poisson process with an average arrival rate of $\lambda_{\mathrm{sM,h}}$ at hour h.

The MVES energy supply rate $g_{\mathrm{s,h}}$ at each station is characterized as the number of PEVs that MVESs can charge simultaneously in an hour. The rate depends on the MVES arrival rate $\lambda_{\mathrm{sM,h}}$, the average MVES discharging capacity $\Delta E_{\mathrm{av.}}$, and average PEV charging demand $L_{\mathrm{av.}}$. It can also be characterized as the summation of incoming MVES energy $E_{\mathrm{Mq_f,h}}$ divided by the average PEV charging demand:

$$g_{\mathrm{s,h}} = \frac{\lambda_{\mathrm{sM,h}} \cdot \Delta E_{\mathrm{av.}}}{L_{\mathrm{av.}}} = \frac{E_{\mathrm{Mq_f,h}}}{L_{\mathrm{av.}}}. \tag{8}$$

Limited capacity station manages the energy coming from MVESs and local feeder together, and then distributes to each charger following the same charging standard.

Assumption 3: The service rate of station s follows an exponential distribution with an average service rate of μ_{s}.

As each station provides charging services to diverse types of PEVs with heterogeneous SoC conditions, the PEV charging service is also a stochastic process. The service time can be modelled as a lognormal distribution based on 2009 NHTS data [25]. To make the service process analytically tractable, we consider that station operators adopt the developed smart charging mechanism in the work [26] to make the service process an exponential distribution. The service rate μ_{s} is related to the adopted charging standard $P_{\mathrm{C,s}}$ and PEV charging demand $L_{\mathrm{av.}}$:

$$\mu_{\mathrm{s}} = \frac{P_{\mathrm{C,s}}}{L_{\mathrm{av.}}}. \tag{9}$$

Based on the above variable modelling, station dynamics in limited capacity station can be characterized as a two-dimensional Markov Chain as shown in Fig. 2.

Each state in the Markov Chain has two parameters, where a denotes the overall number of PEVs being served in the station and b represents the number of PEVs being charged by the energy supplied by MVESs. The number of PEVs being charged by the local feeder is $a - b$.

As the state proceeds horizontally, a increases gradually, denoting that the number of PEVs being served in the station increases. When the state reaches to the right end, it means that all power sources are utilized, and the next incoming PEVs cannot be served. On the other hand, as the state moves vertically, b increases, i.e., the MVES discharging energy increases. Thus, as the row increases, the right-end state in each row denotes a fully occupied station with an increasing MVES discharging capacity. Hence, the summation of the very right states on each row denotes the probability that incoming PEVs will leave without being served at time h, which is considered as the probability of the station unavailability. Complementally, the station availability denotes the probability that incoming PEVs can be charged immediately in the station without additional waiting. The station availability is considered as an essential index of the station power balance condition, which directly affects the station operation performance.

To evaluate the operation performance, the steady-state probabilities of the Markov Chain states need to be obtained. The transition matrix of the Markov Chain M is given as in Equation (10) shown at the bottom of the page. Each element in the model is denoted as $m_{\mathrm{i,j}}$, locating at ith row and jth column. M satisfies $m_{\mathrm{ij}} \geq 0$ (for $i \neq j$) and $m_{\mathrm{ij}} = -\sum_{i=1}^{h} m_{\mathrm{ij}}$ (for $i = j$). l denotes the total number of elements in the Markov Chain, given by,

$$l = \sum_{i=1}^{N_{\mathrm{sM,h}}+1} (N_{\mathrm{sL}} + i). \tag{11}$$

Proposition 1: The Markov Chain is positive recurrent.

Proof: The Markov Chain is irreducible and has finite states, Hence, all states are recurrent [27]. For a finite-state Markov Chain, all recurrent states are positive recurrent [27]. ■

Proposition 2: The Markov Chain has a unique solution for the steady-state probabilities π.

Proof: As a positive recurrent chain, its aperiodic states are ergodic. For an irreducible ergodic Markov Chain in states $i = 0, 1, 2..., h$, steady-state probabilities π exists [27]. ■

In the Markov Chain, π is a $1 \times l$ vector. Let e be an all-one vector of length of l. Through the calculation of balance equations:

$$\begin{cases} \pi \cdot M = 0, \\ \pi \cdot e = 1, \end{cases} \tag{12}$$

$$M = \begin{pmatrix} -(\lambda_{\mathrm{s,h}} + g_{\mathrm{s,h}}) & \lambda_{\mathrm{s,h}} & \dots & g_{\mathrm{s,h}} & 0 & \dots & 0 \\ \mu_{\mathrm{s}} & -(\lambda_{\mathrm{s,h}} + \mu_{\mathrm{s}} + g_{\mathrm{s,h}}) & \dots & 0 & g_{\mathrm{s,h}} & \dots & 0 \\ 0 & 2\mu_{\mathrm{s}} & \dots & 0 & 0 & \dots & 0 \\ \vdots & \vdots & \ddots & \vdots & \vdots & \vdots & \vdots \\ 0 & 0 & \dots & -(\lambda_{\mathrm{s,h}} + g_{\mathrm{s,h}}) & \lambda_{\mathrm{s,h}} & \dots & 0 \\ \mu_{\mathrm{s}} & 0 & \dots & 0 & -(\lambda_{\mathrm{s,h}} + \mu_{\mathrm{s}} + g_{\mathrm{s,h}}) & \dots & 0 \\ \vdots & \vdots & \ddots & \vdots & \vdots & \vdots & \vdots \\ 0 & 0 & \dots & 0 & 0 & \dots & -(N_{\mathrm{s,L}} + N_{\mathrm{sM,h}})\mu_{\mathrm{s}} \end{pmatrix} \tag{10}$$

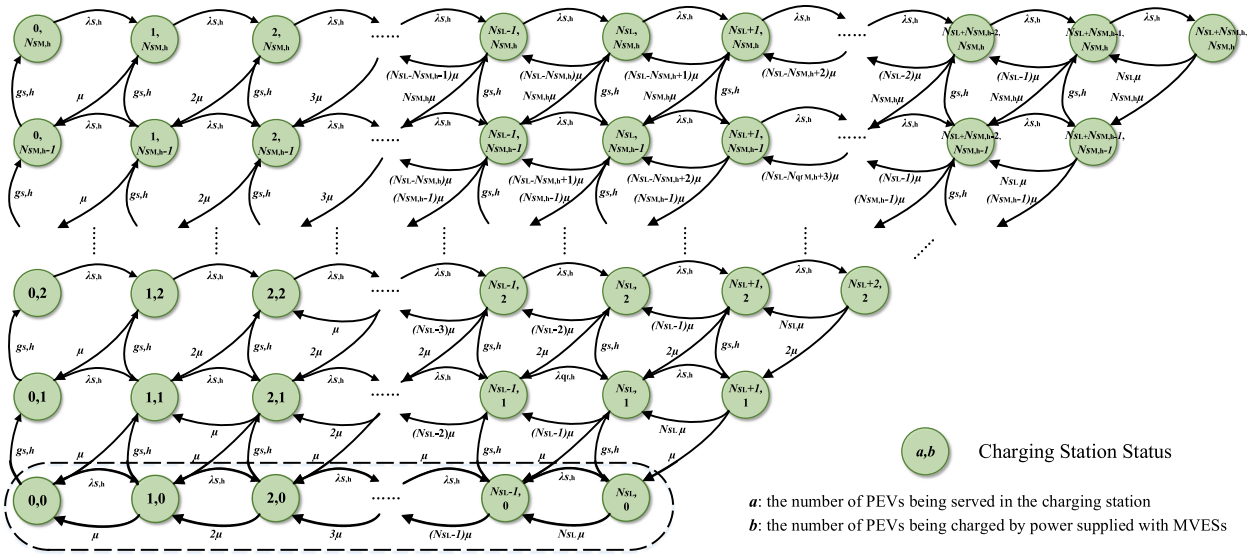

Fig. 2. Hourly Markov Chain with two-dimensional state space.

the steady-state probabilities of Markov can be obtained. Hence, the station unavailability probability can obtained as:

$$p_{\text{unavailability,s,h}} = \sum_{i} \pi_{block}, \tag{13}$$

where

$$\pi_{block} = \{(a,b) : a = N_{\text{s,L}} + i, b = i, i = 0, 1, 2...\}. \tag{14}$$

By contrast, the station availability that is complemental to the unavailability, is denoted as:

$$p_{\text{availability,s,h}} = 1 - p_{\text{unavailbility,s,h}}. \tag{15}$$

When the station availability requirement is set, requested MVES energy can be forecasted using equations (7)–(15).

2) Resourceful Station: Through analyzing the station dynamics in resourceful stations, the MVES charging capacity of the stations can be obtained. PEVs are considered arriving at the station following the same assumption as assumption 1 and the station service process follows assumption 3.

Enabled by sufficient energy supply, resourceful stations do not have MVES discharging in the station. Thus, $g_{\text{s,h}} = 0$ and $N_{\text{sM,h}} = 0$, making the Markov Chain a M/M/N_{sL} queue as dash-lined in Fig. 2.

As the state proceeds horizontally, a increases gradually, denoting that the number of PEVs being served in the station increases. When the state reaches to the right end, it means that all power sources are utilized. Through the calculation of equations (10)–(15), the stationary states of Markov Chain can be obtained. PEV charging demands $R_{\text{s,h}}$ in station s can be calculated as:

$$R_{\text{s,h}} = \sum_{i} \pi_{\text{i}} \cdot m_{\text{i}} \cdot L_{\text{av.}}. \tag{16}$$

Then, the MVES charging capacity of the station is the energy gap between the station overall energy capacity and PEV charging demands, as:

$$C_{\text{Mr}_{\text{e}},\text{h}} = N_{\text{sL}} \cdot L_{\text{av.}} - R_{\text{s,h}}. \tag{17}$$

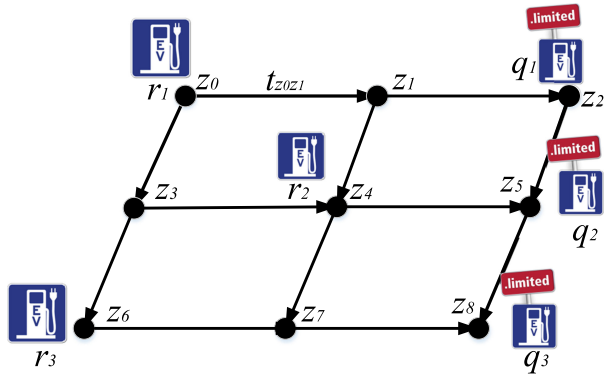

Fig. 3. Transportation network topology of the GCS.

C. Transportation Network Model

The transportation network model, as shown in Fig. 3, consists of road intersections z_{g}, where $\{z_1, z_2 \ldots z_{\text{g}}\} \in Z$ and routes $S_{\text{z}_{\text{m}}\,\text{z}_{\text{n}}}$ between intersections z_{m} and z_{n}. Stations are deployed at intersections. In terms of time variations, traffic velocities fluctuate along routes. The traffic velocities are defined as hourly-average variables between intersections (e.g. $v_{\text{z}_0\,\text{z}_1}$ between intersections z_0 and z_1). The distance between two intersection is denoted as $D_{\text{z}_0\,\text{z}_1}$. Then, the traffic time between two intersections is:

$$t_{\text{z}_0\,\text{z}_1} = \frac{D_{\text{z}_0\,\text{z}_1}}{v_{\text{z}_0\,\text{z}_1}}. \tag{18}$$

A directed graph $G(V, Ed)$ is proposed to model the transportation network model in Fig. 3. V stands for road intersections as vertex, and Ed stands for traffic routes as the graph edges. Traffic time of each route becomes the weight of each

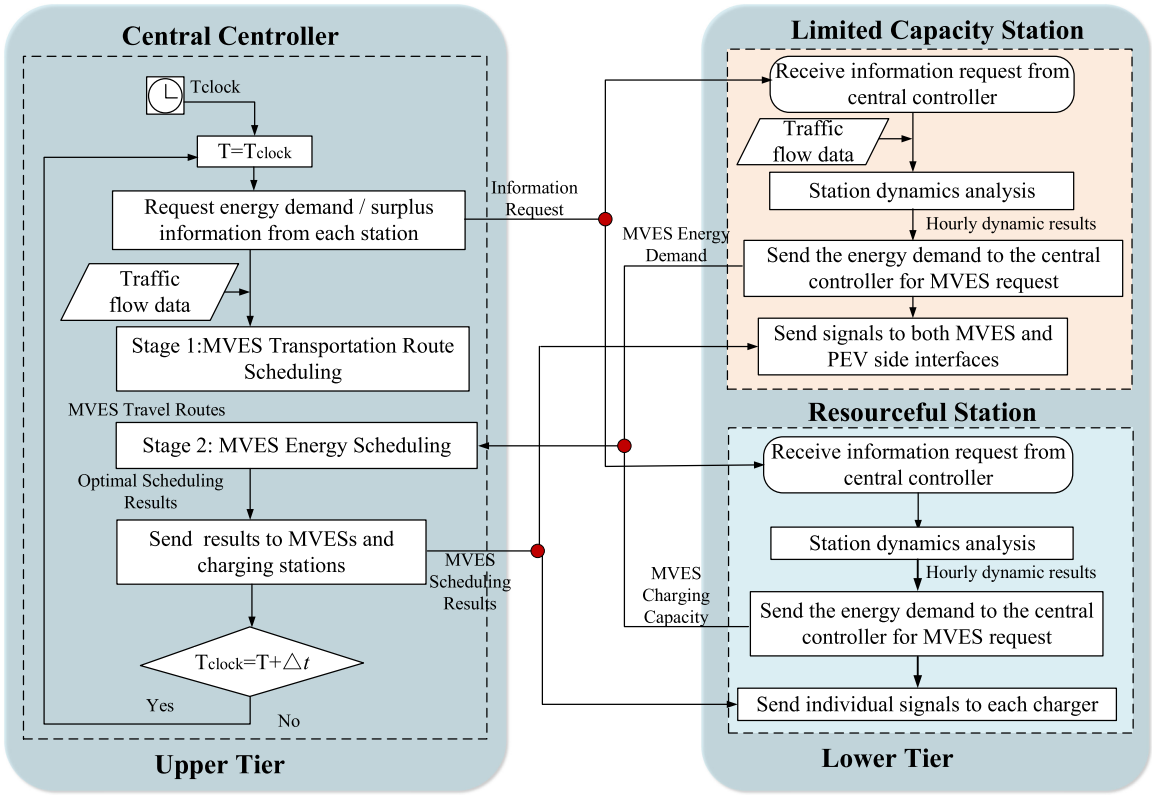

Fig. 4. Flowchart of the two-tier energy compensation framework.

edge. Suppose MVESs that are charged at resourceful charging station r_1 need to transport the surplus energy to limited capacity station q_2, the transmission route can be $S_{z_0 z_1}$-$S_{z_1 z_4}$-$S_{z_4 z_5}$. Considering the traffic variation on road hourly, to enable the time-efficiency of MVES energy transmission along routes, the fastest transmission route is required. For example, when congestion happens on route $S_{z_0 z_1}$, resulting in longer transmission time (larger weight), another transmission route needs to be find. If Routes $S_{z_0 z_3}$-$S_{z_3 z_4}$-$S_{z_4 z_5}$ has the minimal transmission time between stations r_1 and q_2, MVESs will be directed to travel along these routes.

IV. Two-Tier Energy Compensation Framework

To fully utilize the on-road local resources, an energy compensation framework is introduced, as shown in Fig. 4. The framework is operated on two tiers with central controller on the upper tier and charging stations on the lower tier. In terms of fluctuating traffic volumes, the framework operates hourly to provide analysis and guidance for the next-hour operation.

A. Upper Tier Operation

The central controller on the upper tier starts to perform the hourly operation scheme at time T_{clock} by requesting the energy information of each station (e.g. MVES energy demand of limited capacity station and MVES charging capacity of resourceful station). Once the central controller receives the energy demand information from all stations, it starts to schedule MVESs charging and discharging, which consists of two stages:

- *Stage 1. MVES Transportation Route Scheduling:* In terms of collected on-road traffic condition, a route scheduling scheme is conducted to decide the fastest routes between resourceful stations and limited capacity stations so that the time-efficiency of energy transmission can be guaranteed.
- *Stage 2. MVES Energy Scheduling:* Based on the collected energy information, an optimization problem is formulated and solved to arrange the charging and discharging stations for MVES to minimize the overall scheduling costs while maintaining the power balance among all stations.

The scheduling results are then distributed to both resourceful stations and limited capacity stations on the lower tier. The whole process repeats after the time duration Δt of 60 minutes.

B. Lower Tier Operation

- *Limited Capacity Station* q_{f} - Once station q_{f} receives the information request from the upper tier, the station dynamics will be analyzed with the traffic data input. Through the two dimensional Markov Chain analysis, the next-hour energy demand forecast will be obtained and sent to the upper tier. Then, upon receiving the scheduling results from the upper tier, station q_{f} will operate accordingly.

- *Resourceful Station* r_{e} - Upon receiving the information request from central controller, resourceful station r_{e} analyzes the station dynamics and sends its MVES charging capacity to the upper tier as part of the input data for MVES energy scheduling. After receiving the controller scheduling results, r_{e} will then prepare to charge the surplus energy to MVESs.

V. Problem Formulation

Based on the introduced framework, the scheduling problem can be formulated stage by stage.

A. MVES Transportation Route Scheduling

As the framework is operated on an hourly basis, it is essential to enable the time-efficiency of MVES energy transmission. Thus, a fastest path scheduling scheme is proposed to determine the fastest paths between stations in terms of hourly-variant traffic conditions.

Based on the Floyd-Warshall algorithm which finds the fastest travel path between all nodes, we propose the fastest path search scheme as described in Algorithm 1. We first initialize the graph G(V,Ed) with two sets of edge weights: ***time*** for MVES transportation time and ***dist*** for MVES transportation distance. Meanwhile, the hopping nodes ***next*** are initialized as original nodes. As described in line 9-18, the algorithm iteratively chooses one node as hopping node between the origin and destination to find the shortest path. Notably, when the hopping node find a path that has the same weight as the former recorded shortest path, the algorithm will then choose the path that has shorter transportation distance to enable the cost-efficiency of route scheduling (as shown in line 15-18). Further, to output the optimal path results, a path reconstruction scheme is presented from line 20 to 27.

Algorithm 1: Fastest Path search for MVES Energy Transmission.

```
1  Let time be a |V|×|V| array of minimum distance
     initialized to ∞ ;
2  Let dist be a |V|×|V| array of minimum distance
     initialized to ∞ ;
3  let next be a |V|×|V| array of vertex indices initialized
     to null ;
4  Initialization;
5  for each edge (u,v) do
6      time[u][v] ← w_time(u,v) ;
7      dist[u][v] ← w_dist(u,v) ;
8      next[u][v] ← v ;
9  for k from 1 to |V| do
10     for i from 1 to |V| do
11         for j from 1 to |V| do
12             if time[i][j] < time[i][k]+time[k][j] then
13                 time[i][j] ← time[i][k]+time[k][j] ;
14                 next[i][j] ← next[i][k] ;
15             else if time[i][j] = time[i][k]+time[k][j]
                 then
16                 if dist[i][j] < dist[i][k]+dist[k][j] then
17                     time[i][j] ← time[i][k]+time[k][j] ;
18                     next[i][j] ← next[i][k] ;
19 for all edges (u,v) do
20     if u = r_e and v = f then
21         if next[i][j]=null then
22             return [] ;
23         path=[u] ;
24         while u ≠ v do
25             u ← next[i][j]=null ;
26             path.append(u) ;
27         return path ;
```

B. MVES Energy Scheduling

The MVES scheduling is performed on an hourly basis with hourly-averaged performance evaluation. Based on the energy demand forecast, the central controller schedules on-road MVESs aiming at minimizing the overall scheduling costs C_{h} while guaranteeing the power balance. The problem is formulated as follow:

$$\min \quad C_{\mathrm{h}} = C_{\mathrm{charge,h}} + C_{\mathrm{trans.,h}} \tag{19}$$

$$\text{s.t.} \quad p_{\mathrm{availbility,s,h}} \geq p_{\mathrm{QoS,s}}, \forall s \in S \tag{19.a}$$

$$0 \leq E_{\mathrm{r_e,q_f,h}} \leq C_{\mathrm{Mr_e,h}}, \forall r_{\mathrm{e}} \in R, \forall q_{\mathrm{f}} \in Q \tag{19.b}$$

$$\sum_{q_{\mathrm{f}}} E_{\mathrm{r_e,q_f,h}} \leq C_{\mathrm{Mr_e,h}}, \forall q_{\mathrm{f}} \in Q \tag{19.c}$$

$$\sum_{r_{\mathrm{e}}} E_{\mathrm{r_e,q_f,h}} = E_{\mathrm{Mq_f,h}}, \forall r_{\mathrm{e}} \in R \tag{19.d}$$

The scheduling costs C_{h} consists of two parts: the charging costs $C_{\mathrm{charge,h}}$ to charge MVESs with surplus energy at resourceful stations and the transportation costs $C_{\mathrm{trans.,h}}$ of MVESs during their energy transmission processes. The charging costs consist of MVES charging costs at all the resourceful stations, depending on the energy charging price $C_{\mathrm{charge,r_e,h}}(E_{\mathrm{r_e,q_f}})$ at station r_{e} and required MVES energy $E_{\mathrm{r_e,q_f}}$ that sent to limited station q_{f}:

$$C_{\mathrm{charge,h}} = \sum_{r_{\mathrm{e}}} \sum_{q_{\mathrm{f}}} C_{\mathrm{charge,r_e,h}}(E_{\mathrm{r_e,q_f}}) \cdot E_{\mathrm{r_e,q_f}}. \tag{20}$$

As resourceful stations charge incoming PEVs priorly, the remaining energy capacity for MVES charging can be limited, especially in peak charging hours. To characterize the relation between the MVES charging price and demanding MVES energy, a polynomial function is utilized to characterize the price function as:

$$C_{\mathrm{charge,r_e,h}}(E_{\mathrm{r_e,q_f}}) = \alpha_{\mathrm{r_e},1} \cdot E^2_{\mathrm{r_e,q_f}} + \alpha_{\mathrm{r_e},2} \cdot E_{\mathrm{r_e,q_f}} + \alpha_{\mathrm{r_e},3}. \tag{21}$$

The first differential of the function reflects the price deviation relation with demanding MVES energy as:

$$\frac{\mathrm{d}}{\mathrm{d}E_{\mathrm{r_e},\mathrm{q_f}}}\left(C_{\mathrm{charge},\mathrm{r_e},\mathrm{h}}(E_{\mathrm{r_e},\mathrm{q_f}})\right) = 2\alpha_{\mathrm{r_e},1}\cdot E_{\mathrm{r_e},\mathrm{q_f}} + \alpha_{\mathrm{r_e},2}, \quad (22)$$

where $\alpha_{\mathrm{r_e},2}$ denotes the primary price setting without energy fluctuation and $\alpha_{\mathrm{r_e},1}$ represents the price fluctuation causing by the demanding energy deviation from the primary price setting.

In addition to charging in stations, MVES transportation process also incurs electricity and time consumption that is considered as part of scheduling costs. The transportation costs consider factors of distance $D_{\mathrm{r_e q_f}}$ between charging station r_{e} and discharging station q_{f}, the transportation price β per transmission distance per kWh, the transmitted energy $E_{\mathrm{r_e},\mathrm{q_f}}$ along the route $S_{\mathrm{r_e q_f}}$:

$$C_{\mathrm{trans.},\mathrm{h}} = \sum_{r_{\mathrm{e}}}\sum_{q_{\mathrm{f}}} E_{\mathrm{r_e},\mathrm{q_f}}\cdot\beta\cdot D_{\mathrm{r_e q_f}}. \quad (23)$$

While minimizing scheduling costs, every station needs to maintain its power balance by fulfilling most of the arriving PEV charging demands. As shown in constraint (19.a), every charging station needs to guarantee a pre-defined station availability $p_{\mathrm{QoS},\mathrm{s}}$ in the station.

From energy balance perspective, the MVES charging energy $E_{\mathrm{r_e q_f}}$ that is supplied by station r_{e} and sent to station q_{f} should be within the station MVES charging capacity $E_{\mathrm{Mr_e}}$, as in constraint (19.b). The overall MVES charging energy should also be within the station MVES charging capacity, as in constraint (19.c). On the MVES energy supply side, the summation of arriving MVES energy at station q_{f} should equals to its demanding energy $E_{\mathrm{Mq_f},\mathrm{h}}$, as denoted in constraint (19.d).

The formulated problem is convex in nature with a convex set that can be efficiently solved through Disciplined Convex Programming (DCP) of CVX [34]. Through the DCP ruleset examination, the convexity of formulated problem can be validated. Then, the continuous functions as our formulated ones can be solved through simple convex programming implementation using atom library (regulated convex or concave functions). The whole process of MVES scheduling is described as Algorithm 2 . After hourly traffic data input and initialization, the MVES energy demand and charging capacity calculation are conducted though Markov Chains respectively. Based on the collected traffic data, MVES energy transmission routes are planned by the fastest path search scheme of Algorithm 1. Then, DCP is conducted to minimize scheduling costs provided the transmission routes, energy demands, and requests.

VI. Simulation Results

In this section, the effectiveness of the introduced framework is evaluated based on the real traffic data on California highway collected by the California department of transportation. Further, impacts of station availability and transportation cost on framework results are discussed.

Algorithm 2: Energy Compensation Framework.

Input: Hourly traffic flow;
Hourly transportation time of each route ;

Initialization
Let h=0
Let $E_{\mathrm{Ms,h}}$=0, $R_{\mathrm{s,h}}$=0 ;
for *h=0 to 23* **do**
  Markov Chain Analysis:
  Calculate MVES energy demand $E_{\mathrm{Mq_f,h}}$ of limited station q_{f};
  Calculate MVES charging capacity $E_{\mathrm{Mr_e,h}}$ of resourceful station r_{e} ;
  Do *fastest path search scheme* for MVES energy transportation ;
  Output: Fastest transportation routes between stations ;
  DCP for cost-minimized MVES energy scheduling:
  DCP ruleset examination;
  DCP simple implementation ;
  Output: MVES energy allocation results to all stations
  Energy allocation and transportation path to all MVESs.

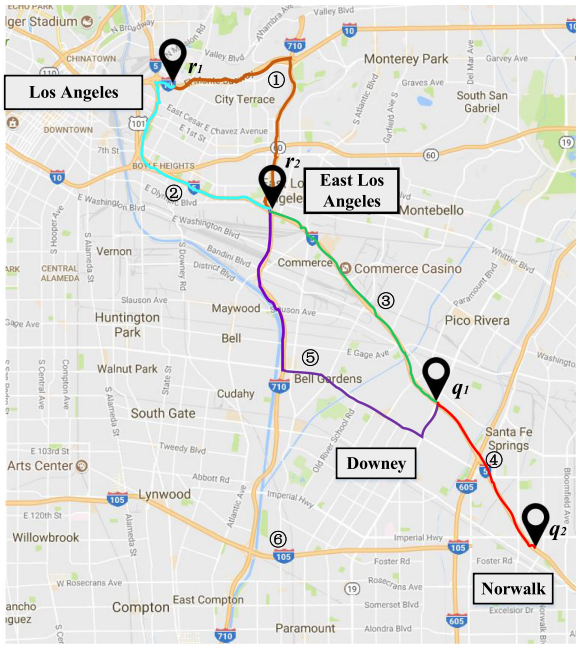

Fig. 5. Charging station deployment in South California.

A. Simulation Setup

To evaluate the performance of the introduced framework, simulation is conducted based on the California highway data collected by the California department of transportation PeSM [32]. As shown in Fig. 5, the MVES travelling area covers from downtown Los Angeles (L.A.) to Norwalk, with four charging stations deployed along unidirectional highway I-5S. Resourceful stations r_1 and r_2 are deployed near downtown L.A. and

TABLE I
ROUTE INFORMATION

Departure	*Destination*	*Travel Highway*	*Route Number*	*Mileage* (km)	*Color*
L. A. DT	East L. A.	I-10E, I-710S	1	10.6	Brown
L. A. DT	East L. A.	I-5S	2	8.1	Blue
East L. A.	Downey	I-5S	3	8	Green
Downey	Norwalk	I-5S	4	8	Red
East L. A.	Downey	I-710S, Local	5	16	Purple

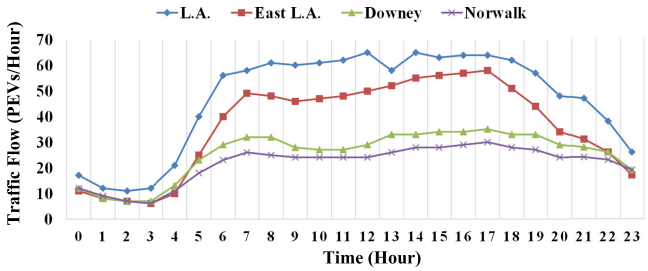

Fig. 6. PEV hourly arrival rate at each station.

East L.A. respectively. To satisfy the huge electricity demand in the urban area, large-capacity feeders and bulk generations are accessible to these two stations. Limited capacity stations q_1 and q_2 are located at Downey and Norwalk respectively. In terms of transportation conditions, we select five major travel routes connecting stations, with details shown in Table I.

1) PEV Settings: A 10% PEV market share in the vehicle market is considered. For resourceful stations, 10% of the on-road PEVs enter stations for recharging. 5% PEVs are recharged at the limited capacity stations. Hence, the PEV arrival rate at each station are shown in Fig. 6.

Connecting to large-capacity feeders, resourceful stations have large feeder capacity with fast charging speed. Station r_1 has a power capacity C_{r_1} of 2.4 MWh while r_2 can provide energy C_{r_2} up to 1.8 MWh [4]. For the limited capacity stations that connect to secondary feeders in domestic area, power supply capacities reduce to hundred-kW level with lower voltage between 100–240 V [4]. In this case, we consider that station q_1 can provide a maximum energy $C_{\mathrm{q}_1\mathrm{L}}$ at 480 kWh and station q_2 has a feeder capacity $C_{\mathrm{q}_2\mathrm{L}}$ of 300 kWh. Charging stations adopt different charging standards to fit the local conditions. For example, resourceful stations use the SAE CCS level 3 standard [29] to charge PEVs at 120 kW while limited capacity stations adopt the SAE CCS level 2 at 90 kW [29]. To ensure that resourceful stations accomplish their PEV charging tasks prior to charging MVESs, the station availability needs to maintain at 95% so that 95% of incoming PEVs will be charged immediately in the station. On the other hand, limited capacity stations should be able to fulfill 90% of incoming PEV charging demands with MVES scheduling. The MVES charging cost coefficients $\alpha_{\mathrm{re},1}, \alpha_{\mathrm{re},2}$ are set as in Table III to map with the current electricity rate plan of Pacific Gas and Electric (PGE) company in California [33]. The coefficient of transportation cost β is set to 0.004 [30]. The parameter settings are also summarized in Table III.

2) Route Choice: First, the fastest routes are palnned by the proposed fastest path search algorithm for MVES energy transmission, as below. The algorithm inputs data of routes travelling time are extracted from google map [31] on an hourly basis, as summarized in Table II.

- **L.A. - Downey**:
  - *12 a.m.-14 p.m. and 19 p.m.-23 p.m.*: Route 1 - Route 3;
  - *15 p.m.-18 p.m.*: Route 2 - Route 3;
- **L.A. - Norwalk:**:
  - *12 a.m.-14 p.m. and 19 p.m.-23 p.m.*: Route 2 - Route 3 - Route 4;
  - *15 p.m.-18 p.m.*: Route 1 - Route 3 - Route 4;
- **East L.A. - Downey**: Route 3 All day;
- **East L.A. - Norwalk**: Route 3 - Route 4 All day;

B. Simulation Results

Solving the optimization problem through proposed scheme on MATLAB platform, we can obtain the optimal MVES scheduling results. First, the improvement of station availability is validated to show that MVESs have been effectively assigned to GCS to enable energy balance. As the objective of the proposed scheme is to mitigate the overload issues of GCS with minimal costs, the overload mitigation is then illustrated through the result comparison of demanding energy from local feeder with and without MVES participation. Finally, the cost comparison results between the proposed scheme and randomly-assigned case are presented.

1) Station Availability: Comparisons of station availabilities before and after MVES scheduling are shown in Fig. 7. As shown in Fig. 7 (a), without MVES scheduling, the availability of station q_1 at Downey encounters enormous drop during the daytime from 6 a.m. to 11 p.m.. That is, depending solely the on local wired power supplement, the station encounters service congestion (i.e. more than 10% of arriving PEVs cannot be served immediately) when more than 20 PEVs come to the station. During the daytime, traffic flow near Downey fluctuates between 23 to 35 PEVs/hour as in Fig. 6, causing the station consistently congested. After MVESs being scheduled to the station, the availability of the station remains stably around 90%.

Similarly, in Fig. 7 (b), the availability of station q_2 at Norwalk has effective improvement during the daytime between 6 a.m. to 11 p.m.. As MVESs are scheduled to station q_2 corresponding to the station required charging demand, the station availability remains stably around 90%.

2) Overload Mitigation Through MVES Scheduling: local feeder to guarantee a 90% station availability is presented in Fig. 8. The results are compared between the case with and without MVES scheduling to verify the significance of MVES participation. Without MVES scheduling, the demanding energy from the local feeder at station 1, as shown in Fig. 8 (a), starting to dramatically increase at 5 a.m., due to the increasing vehicle traffics. Without MVES scheduling and proper infrastructure

TABLE II
AVERAGE TRAVEL TIME OF ROUTES

Time (hr)	0	1	2	3	4	5	6	7	8	9	10	11	12	13	14	15	16	17	18	19	20	21	22	23
Route 1 (min)	10	10	12	12	10	10	9	10	11	11	11	11	12	12	16	16	16	16	14	10	10	10	12	10
Route 2 (min)	7	7	7	7	8	7	8	9	10	10	10	9	10	12	16	22	24	22	18	10	8	9	8	8
Route 3 (min)	7	8	8	8	8	8	8	8	9	8	8	9	10	12	14	20	22	24	22	16	12	10	8	7
Route 4 (min)	5	5	5	5	5	5	7	6	7	7	7	7	7	8	9	10	12	12	12	10	10	7	6	5
Route 5 (min)	14	14	14	14	14	14	16	18	20	18	18	20	18	22	25	30	35	40	40	30	18	17	16	14

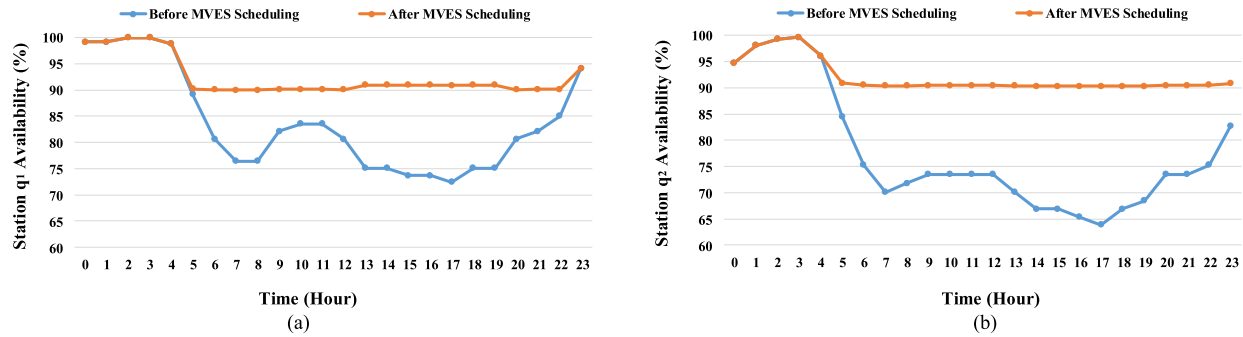

Fig. 7. Station availability comparison.

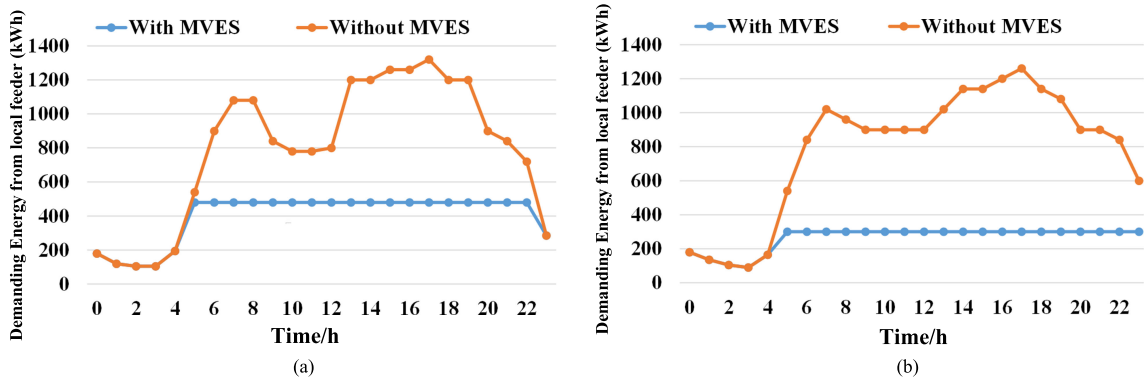

Fig. 8. Demanding energy of local feeder.

TABLE III
SIMULATION PARAMETERS

Para.	Value	Para.	Value
C_{r_1}	2.4 MWh	C_{r_2}	1.8 MWh
$C_{\mathrm{q}_1\mathrm{L}}$	480 kWh	$C_{\mathrm{q}_2\mathrm{L}}$	300 kWh
$\mu_{\mathrm{r_e}}$	120 kW	$\mu_{\mathrm{q_f}}$	90 kW
$P_{\mathrm{C,r_e}}$	120 kW	$P_{\mathrm{C,q_f}}$	90 kW
$\rho_{\mathrm{r_e,h}}$	1%	$\rho_{\mathrm{q_f,h}}$	0.5%
$\alpha_{\mathrm{r}_1,1}$	0.000167	$\alpha_{\mathrm{r}_1,2}$	0.0332
$\alpha_{\mathrm{r}_2,1}$	0.00025	$\alpha_{\mathrm{r}_2,2}$	0
β	0.004		

upgrade, the demanding energy exceeds the limit of local feeder capacity during daytime, which can severely overload the feeder. With MVES scheduling, local feeder only needs to provide energy up to its capacity limit (480 kWh). Hence, with MVES participation, the potential overload issue is effectively mitigated at station 1.

Similar to station 1, station 2 also encounters severe power overload during daytime. As shown in Fig. 8 (b), starting from 5 a.m., demanding energy from local feeder can peak up to 1200 kWh without MVES scheduling. With only 300 kWh feeder capacity, the peak hour PEV charging demand can easily crash the normal power operation and cause severe transformer degradation. On the other hand, with MVES participation, local feeder only needs to provide its feeder capacity value during daytime to effectively avoid the potential overloading.

3) MVES Scheduling Costs: To illustrate the optimality of the proposed cost minimization scheme, a randomly-arranged MVES scenario is presented as the baseline case. The scheduling cost performance in Fig. 9 (a), shows that through the proposed cost-minimized scheduling scheme, the scheduling cost can be

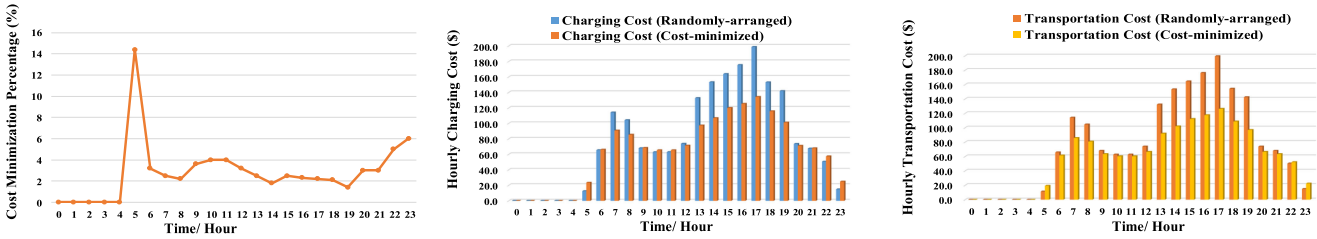

Fig. 9. MVES scheduling cost performance comparison.

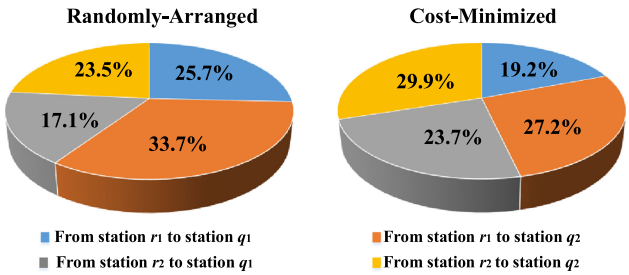

Fig. 10. MVES charging task allocation comparison.

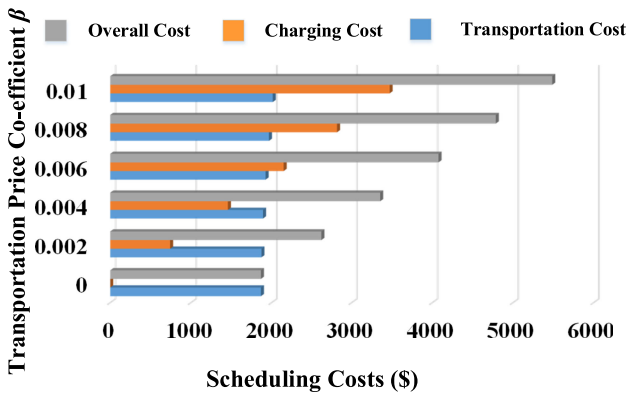

Fig. 11. MVES scheduling costs with transportation price co-efficient.

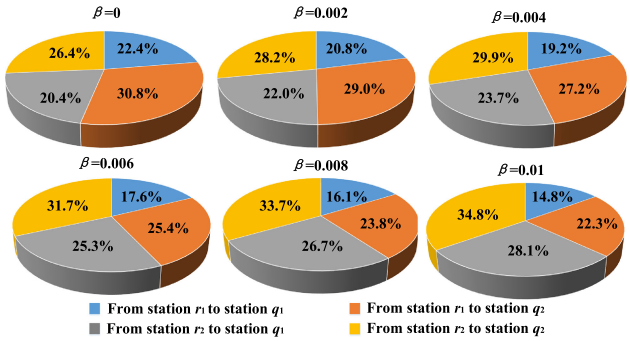

Fig. 12. MVES charging task allocation with transportation price co-efficient.

effectively minimized hourly from 6 a.m. to 11 p.m.. As part of the scheduling costs, charging cost has been effectively reduced in most of the time other than 10–11 a.m. and 9–11 p.m.. This situation incurs as transportation cost outweighs charging cost when both of the resourceful stations have sufficient energy to cope with MVES charging tasks. Compared with station r_1 that has lower charging price but longer transportation distance, station r_2 will be assigned with more charging tasks. The transportation cost is also minimized as shown in Fig. 9 (c), by flexibly arranging the MVES energy tasks among resourceful stations.

Fig. 10 shows the hourly-averaged charging tasks from stations r_{e} to stations q_{f} of both cost-minimized and randomly-arranged cases. Randomly-arranged case assigns more charging tasks to station r_1 considering its large charging capacity. However, when transportation cost is addressed in the cost-minimized case, MVES charging tasks are allocate more to station r_2 to minimize MVES transportation distance, which is in accordance with the practical concerns of minimizing transportation cost.

4) Influence of MVES Transportation Cost: As the electric battery technology advances, charging and discharging price per energy unit of MVESs will decrease correspondingly, leading to an decrease of MVES transportation price. The fluctuation of MVES transportation price has the potential to affect scheduling decisions. In this subsection, the transportation price co-efficient β is used as the reflection of price evolution to illustrate the transportation cost influence on scheduling results.

Fig. 11 shows that as β increases, the overall scheduling cost increases. The increment of β, leading to the transportation cost increase, accounts for a heavy proportion of the whole cost. Although the MVES charging demand is irrelevant to transportation routes, the transportation price coefficient does affect the MVES charging task allocation, which leads to an slightly increasing charging cost.

To illustrate the influence of β on MVES charging allocation, Fig. 12 shows the charging allocation trends as β increases. It can be seen that transportation price increment results in the decrease of MVES charging tasks in station r_1 as the station is the farther one to both limited capacity stations. Particularly, MVESs that go to station q_1 tend to be allocated to station r_2 due to a shorter transportation distance. Although r_2 is closer to both limited capacity stations, its higher charging cost and limited charging capacity require station r_1 to share some charging responsibility to ensure that enough MVESs will arrive at the limited capacity stations on time.

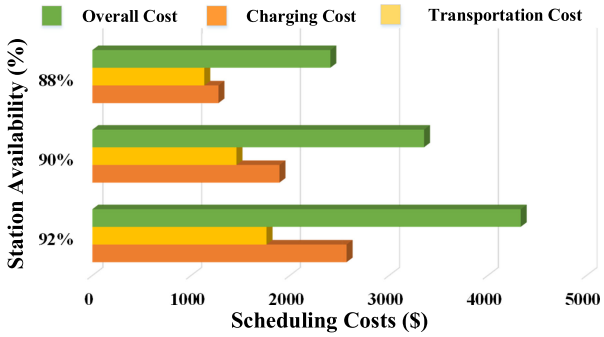

Fig. 13. MVES scheduling costs with station availability.

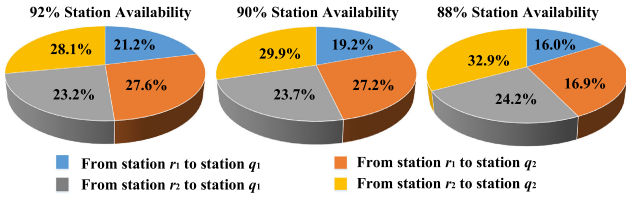

Fig. 14. MVES charging task allocation with station availability.

5) Station Availability vs. MVES Scheduling Costs: In the limited capacity stations, the requirement of station availability has non-negligible impacts on MVES scheduling costs and charging task allocations among resourceful stations. Fig. 13 shows daily MVES scheduling cost variations with limited capacity station availability. With higher station availability requirement, the overall scheduling cost increases rapidly. To maintain a higher station availability, more energy are demanded to be transferred through MVESs. Thus, charging tasks increase in resourceful stations, leading to higher charging cost. On the other hand, maintaining a higher station availability also results in an increase of MVES transportation cost. The detailed charging allocations with increasing station availability are illustrated in Fig. 14. It can be seen that higher the station availability, more MVES charging tasks are assigned to station r_1. Considering a smaller charging capacity in station r_2 between the two resourceful stations, fulfilling the increasing charging tasks means allocating more MVES charging to station r_1.

VII. Conclusion

A two-tier energy compensation framework has been introduced to effectively use MVESs as energy porters at peak hours. To minimize the scheduling cost, a convex optimization problem has been formulated and solved through DCP of CVX. Through the simulation, the effectiveness of the introduced framework and the optimality of formulated problem have been validated. Moreover, the influence of scheduling factors on the framework results have been illustrated. It is concluded that as battery technology develops, the increasing MVES energy transmission efficiency can lead to a wider transmission coverage and more flexible scheduling. Further, strict station availability requirement can result in drastic increment of scheduling cost, leading to a trade-off between the station availability and scheduling costs. Based on the introduced energy compensation framework, the cost-efficient MVES scheduling scheme can be applied to the local power utility company to address the overload issues without excessive facility upgrade expenditure. In our future work, we will propose an incentive mechanism to encourage private MVESs participating in the energy compensation scheduling to fully utilize the on-road energy sources.

References

[1] K. Hartman, State efforts promote hybrid and electric vehicles, 2015. [Online]. Available: http://www.ncsl.org/research/energy/stateelectric-vehicle-incentives-state-chart.aspx

[2] K. Lindquist and M. Wendt, "Electric vehicle policies, fleet, and infrastructure: Synthesis," Washington State Dept. Trans., Tacoma, WA, USA, Tech. Rep. DOE/EIA-0484(2011), Nov. 2011.

[3] N. Chen, M. Wang, N. Zhang, X. Shen, and D. Zhao, "SDN based framework for the PEV integrated smart grid," *IEEE Netw.*, vol. 31, no. 2, pp. 14–21, Mar. 2017.

[4] H. Xiao, Y. Huimei, and W. Chen, "A survey of influence of electrics vehicle charging on power grid," in *Proc. 9th IEEE Conf. Ind. Electron. Appl.*, Hangzhou, Zhejiang, Jun. 2014, pp. 121–126.

[5] M. Wang *et al.*, "Asymptotic throughput capacity analysis of VANETs exploiting mobility diversity," *IEEE Trans. Veh. Technol.*, vol. 64, no. 9, pp. 4187–4202, Sep. 2015.

[6] H. Peng *et al.*, "Resource allocation for cellular-based inter-vehicle communications in autonomous multiplatoons," *IEEE Trans. Veh. Technol.*, vol. 66, no. 12, pp. 11249–11263, Dec. 2017.

[7] W. Su, H. Rahimi-Eichi, W. Zeng, and M. Chow, "A survey on the electrification of transportation in a smart grid environment," *IEEE Trans. Ind. Inform.*, vol. 8, no. 1, pp. 1–10, Feb. 2012.

[8] S. Townsend, Ontario Canada helps electric vehicle drivers plug in, 2013. [Online]. Available: http://www.altenergymag.com/content.php?posttype=2037

[9] C. M. Martinez, X. Hu, D. Cao, E. Velenis, B. Gao, and M. Wellers, "Energy management in plug-in hybrid electric vehicles: Recent progress and a connected vehicles perspective," *IEEE Trans. Veh. Technol.*, vol. 66, no. 6, pp. 4534–4549, Jun. 2017.

[10] W. Kempton and J. Tomic, "Vehicle-to-grid power fundamentals: Calculating capacity and net revenue," *J. Power Sources*, vol. 144, no. 1, pp. 268–279, Jun. 2005.

[11] A. Lam, K.-C. Leung, and V. O. K. Li, "Capacity estimation for vehicle-to-grid frequency regulation services with smart charging mechanism," *IEEE Trans. Smart Grid*, vol. 7, no. 1, pp. 156–166, Jan. 2016.

[12] S. Han, S. Han, and K. Sezaki, "Estimation of achievable power capacity from plug-in electric vehicles for V2G frequency regulation: Case studies for market participation," *IEEE Trans. Smart Grid*, vol. 2, no. 4, pp. 632–641, Aug. 2011.

[13] R. Wang, Y. Li, P. Wang, and D. Niyato, "Design of a V2G aggregator to optimize PHEV charging and frequency regulation control," in *Proc. IEEE Int. Conf. Smart Grid Commun.*, Vancouver, BC, Canada, Dec. 2013, pp. 127–132.

[14] J. J. Escudero-Garzás, A. García-Armada, and G. Seco-Granados, "Fair design of plug-in electric vehicles aggregator for V2G regulation," *IEEE Trans. Veh. Technol.*, vol. 61, no. 8, pp. 3406–3419, Aug. 2012.

[15] H. Liang, B. J. Choi, W. Zhuang, and X. Shen, "Optimizing the energy delivery via V2G systems based on stochastic inventory theory," *IEEE Trans. Smart Grid*, vol. 4, no. 4, pp. 2230–2243, Jul. 2013.

[16] H. Khayyam, J. Abawajy, B. Javadi, A. Goscinski, A. Stojcevski, and A. Bab-Hadiashar, "Intelligent battery energy management and control for vehicle-to-grid via cloud computing network," *Appl. Energy*, vol. 111, pp. 971–981, Nov. 2013.

[17] V. N. Coelho *et al.*, "Multiobjective energy storage power dispatching using plug-in vehicles in a smart-microgrid," *Renew. Energy*, vol. 89, pp. 730–742, Apr. 2016.

[18] P. Yi, T. Zhu, B. Jiang, B. Wang, and D. Towsley, "An energy transmission and distribution network using electric vehicles," in *Proc. IEEE Int. Conf. Commun.*, Ottawa, ON, Canada, Jun. 2012, pp. 3335–3339.

[19] P. Yi *et al.*, "Renewable energy transmission through multiple routes in a mobile electrical grid," in *Proc. IEEE PES Innovative Smart Grid Technol.*, Washington DC, USA, Feb. 2014, pp. 1–5.

[20] M. Wang, M. Ismail, R. Zhang, X. Shen, E. Serpedin, and K. Qaraqe, "Spatio-temporal coordinated V2V fast charging strategy for mobile GEVs via price control," *IEEE Trans. Smart Grid*, vol. 9, no. 3, pp. 1566–1579, May 2018.
[21] T. D. Atmajaa and M. Mirdanies, "Electric vehicle mobile charging station dispatch algorithm," in *Proc. 2nd Int. Conf. Sustain. Energy Eng. Appl.*, West Java, Indonesia, Oct. 2014, pp. 326–335.
[22] I. S. Bayram, G. Michailidis, M. Devetsikiotis, and F. Granelli, "Electric power allocation in a network of fast charging station," *IEEE J. Sel. Areas Commun.*, vol. 31, no. 7, pp. 1235–1246, Jul. 2013.
[23] N. Wisitpongphan, F. Bai, P. Mudalige, V. Sadekar, and O. Tonguz, "Routing in sparse vehicular ad hoc wireless networks," *IEEE J. Sel. Areas Commun.*, vol. 25, no. 8, pp. 1538–1556, Oct. 2007.
[24] Nissan Leaf 2017, 2017. [Online]. Available: http://www.nissan.ca/en/electric-cars/leaf/charging-range/
[25] A. Santos, N. McGuckin, H. Y. Nakamoto, D. Gary, and S. Liss, "Summary of travel trends: 2009 national household travel survey," U.S. Dept. Transp., Washington, DC, USA, Tech. Rep. FHWA-PL-ll-022, Jun. 2011.
[26] A. L. S. Lam, K. Leung, and V. O. K. Li, "Capacity estimation for vehicle-to-grid frequency regulation services with smart charging mechanism," *IEEE Trans. Smart Grid*, vol. 7, no. 1, pp. 156–166, Jan. 2016.
[27] H. M. Taylor and S. Karlin, "Continuous time Markov Chain," in *An Introduction to Stochastic Modeling*, 3rd ed. San Diego, CA. USA: Academic, 2014, pp. 333–408.
[28] D. Ban, G. Michailidis, and Mi. Devetsikiotis, "Demand response control for PHEV charging stations by dynamic price adjustments," in *Proc. IEEE PES Innovative Smart Grid Technol.*, Washington DC, USA, Jan. 2012, pp. 1–8.
[29] *SAE Electric Vehicle and Plug in Hybrid Electric Vehicle Conductive Charge Coupler*, SAE Standard J1772, 2012.
[30] R. Alvaro-Hermana, J. Fraile-Ardanuy, P. J. Zufiria, L. Knapen, and D. Janssens, "Peer to peer energy trading with electric vehicles," *IEEE Trans. Intell. Transp. Syst.*, vol. 8, no. 3, pp. 33–44, Fall 2016.
[31] Google Map, 2017. [Online]. Available: https://www.google.ca/maps
[32] Caltrans PeMS, 2018. [Online]. Available: http://pems.dot.ca.gov
[33] Electric Vehicle rate plans, 2018. [Online]. Available: https://www.pge.com
[34] CVX Research, Inc., CVX: Matlab software for disciplined convex programming, version 2.0, Apr. 2011. [Online]. Available: http://cvxr.com/cvx

Nan Chen (S'15) received the Bachelor's degree in electrical and control engineering from Nanjing University of Aeronautics and Astronautics, Nanjing, China, in 2014. She is currently working toward the Ph.D. degree in electrical and computer engineering from the University of Waterloo, Waterloo, ON, Canada. Her current research interests include electric vehicle charging scheduling and V2G application in smart grid.

Jinghuan Ma (S'15) received the B.S. degree in electronic engineering and the Ph.D. degree in signal and information processing from Peking University, Beijing, China, in 2013 and 2018, respectively. He was a Visiting Scholar with the Broadband Communications Research Group, University of Waterloo, Waterloo, ON, Canada, from 2016 to 2017. His research interests include energy Internet and scheduling in smart grid and wireless communications.

Miao Wang (M'15) received the B.Sc. degree from the Beijing University of Posts and Telecommunications, Beijing, China, and the M.Sc. degree from Beihang University, Beijing, Beijing, China, in 2007 and 2010, respectively, and the Ph.D. degree in electrical and computer engineering from the University of Waterloo, Waterloo, ON, Canada, in 2015. She is an Assistant Professor with the Department of Electrical and Computer Engineering, Miami University, Oxford, OH, USA. Her current research interests include electric vehicles charging/discharging strategy design in smart grid, traffic control, capacity and delay analysis, and routing protocol design for vehicular networks.

Xuemin (Sherman) Shen (M'97–SM'02–F'09) received the B.Sc. degree from Dalian Maritime University, Dalian, China, in 1982, and the M.Sc. and Ph.D. degrees from Rutgers University, New Brunswick, NJ, USA, in 1987 and 1990, respectively, all in electrical engineering. He is a University Professor and the Associate Chair for Graduate Studies, Department of Electrical and Computer Engineering, University of Waterloo, Waterloo, ON, Canada. His research interests include resource management, wireless network security, social networks, smart grid, and vehicular ad hoc and sensor networks. He served as the Technical Program Committee Chair/Co-Chair for the IEEE Globecom'16, Infocom'14, the IEEE VTC'10 Fall, and Globecom'07, the Symposia Chair for the IEEE ICC'10, the Tutorial Chair for the IEEE VTC'11 Spring and the IEEE ICC'08, the General Co-Chair for ACM Mobihoc'15, Chinacom'07 and the Chair for the IEEE Communications Society Technical Committee on Wireless Communications. He also serves/served as the Editor-in-Chief for the IEEE INTERNET OF THINGS JOURNAL, the IEEE NETWORK, *Peerto-Peer Networking and Application*, and IET Communications; a Founding Area Editor for the IEEE TRANSACTIONS ON WIRELESS COMMUNICATIONS; an Associate Editor for THE IEEE TRANSACTIONS ON VEHICULAR TECHNOLOGY, Computer Networks, *ACM/Wireless Networks*, etc.; and the Guest Editor for the IEEE JSAC, IEEE WIRELESS COMMUNICATIONS, the IEEE COMMUNICATIONS MAGAZINE, etc. He was a recipient of the Excellent Graduate Supervision Award in 2006, and the Premiers Research Excellence Award in 2003 from the Province of Ontario, Canada. He is a registered Professional Engineer of Ontario, Ontario, ON, Canada, an Engineering Institute of Canada Fellow, a Canadian Academy of Engineering Fellow, a Royal Society of Canada Fellow, and a Distinguished Lecturer for the IEEE Vehicular Technology Society and Communications Society.